# Chapter 2
# Theory Framework: QCD

The theoretical framework of particle physics is called the Standard Model (SM). The SM is a SU(3)⊗ SU(2)⊗ U(1) gauge theory, describing the strong (QCD), weak and electromagnetic interactions respectively. It describes the interactions of the fundamental components of matter, quarks, leptons and gauge bosons, according to three of the four forces in nature. Measurements of the Standard Model parameters have confirmed the theoretical predictions to increasing precision, but evidence that new physics phenomena are needed to extend the knowledge of the fundamental components of matter could be found at the LHC.

This chapter outlines the theoretical framework that underlies the measurement described in this thesis, and the tools used to simulate hadron interactions for the theoretical predictions used for comparison with the measurement. An overview of the Standard Model in terms of the electroweak interactions is given in Sect. 2.1. A brief description of the Quantum Chromodynamics concepts used in this thesis follows in Sect. 2.2. Section 2.3 introduces the concept of jets as tools to obtain predictable and measurable quantities and the motivations to measure the inclusive jet cross section. Finally Sect. 2.4 outlines the theoretical and computational tools used for the simulation of hadronic interactions.

## 2.1 Introduction to the Standard Model

The Standard Model is the theoretical framework that describes strong, weak and electromagnetic interactions between fundamental particles (see [1–4] for a concise introduction and further references). It is a non-abelian gauge theory: the transformations of the symmetry group do not commute in the case of the QCD and weak groups. Gauge invariance, defined as the invariance of the theory under local transformations, is a fundamental property of the theory. Gauge invariance defines the particle content of the Standard Model (as shown in Fig. 2.1), as the quanta of the gauge invariant fields are identified with the five gauge bosons. These are the photon,

C. Doglioni, *Measurement of the Inclusive Jet Cross Section with the ATLAS Detector at the Large Hadron Collider*, Springer Theses,
DOI: 10.1007/978-3-642-30538-2_2, 

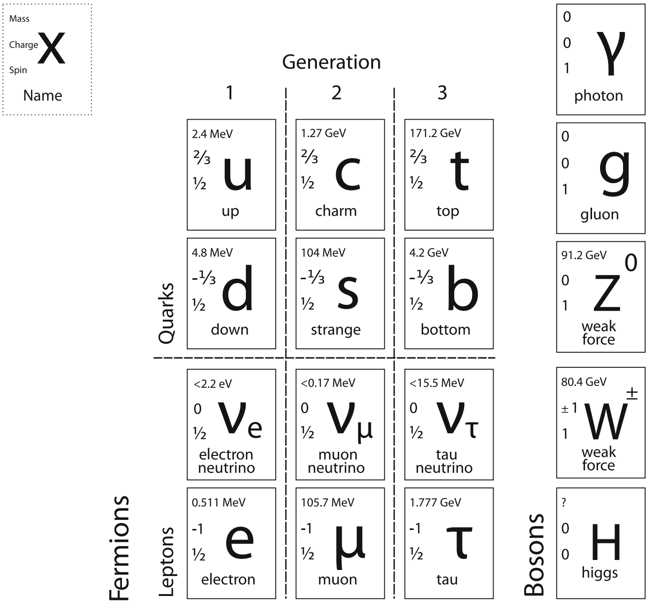


**Fig. 2.1** The fundamental particles of the Standard model, sorted according to family, generation and mass. Figure from [7]

the gluon, the $W^{+/-}$ and Z and they act as mediators of the forces. A consequence of the non-abelian character of the theory is that the gauge bosons for the QCD and weak forces enjoy self-interactions. In addition to the gauge bosons, the Standard Model is composed of 12 fermions of spin 1/2, grouped in three lepton and three quark families. These are considered point-like, as there is no evidence of any internal structure of leptons or quarks to date. The mass of the Standard Model particles can be introduced using the Higgs mechanism [5, 6] through spontaneous symmetry breaking that leads to the appearance of a new boson. The Higgs boson has not yet been observed, and its discovery is sought by the general purpose experiments at the Large Hadron Collider.

## 2.2 Key Concepts in Quantum Chromodynamics

Quantum chromodynamics is the theory of strong interactions. Its fundamental actors are quarks and gluons, which are confined in the nucleon but act as free at sufficiently small scales (and high energies). The latter behaviour is called *asymptotic freedom*. The direct consequence of confinement is that free quarks and gluons are never observed experimentally, and their final state is a collimated shower of hadrons.

The development of QCD was posterior to that of QED: while the latter was highly successful in the mid-Sixties, no information about the components of the nucleons was available, and strong interactions were commonly described using general principles and the exchange of mesons [8] although the basis for theories that could eventually accommodate QCD had also been developed [9].

A framework called *Eightfold Way* [10] had been developed to organize subatomic baryons and mesons into octets. Its connection to an underlying pointlike structure of hadrons came after the so-called *heroic age* of deep inelastic scattering measurements interpreted using the parton model [11]. These experiments and subsequent interpretations showed that the probes scattered against pointlike, spin 1/2 constituents of the nucleons that are the quarks (some relevant papers are collected in Ref. [12]). The presence of spin 1 gluons was also inferred using kinematic considerations in terms of the total momentum shared by the quarks. The QCD equivalent of the electromagnetic charge for QCD is the *colour charge*: (anti)quarks can take three (anti)colours (red, green and blue and their counterparts) while the eight interacting gluons exist in a superposition of colour and anticolour states.

SU(3) QCD was established as a theoretical framework for strong interactions only following the discovery of asymptotic freedom as a consequence of the theory's renormalisability [13]. These concepts will be explored further in the following section. Only a brief overview of the concepts and formulas directly used in this thesis is given, while more material is available in the references quoted.

### 2.2.1 Asymptotic Freedom and Confinement

Gluons in QCD are massless, therefore the theory contains divergences that manifest themselves as infinite results in theoretical cross section calculations. A renormalisation procedure is necessary in order to allow the theory to give meaningful (non infinite) results that can be compared to the experimental measurements. This is achieved by effectively subtracting these infinities through counterterms embedded in so-called *bare* parameters that are not measurable. The renormalisation procedure introduces a correction to the 'renormalised parameter' depending on the renormalisation scale $\mu_R$ (that can be interpreted as the scale at which the subtraction is made) and on the physical scale at which the measurement is made, taken as the squared momentum transfer $Q^2$ in the following. Imposing the independence of the final result (all orders of perturbation theory) from the renormalisation scale allows one to derive an explicit form for the renormalised parameter.[1] As an example of a renormalised parameter, the strong coupling constant is shown in Eq. 2.1:

$$\alpha_s(Q^2) = \frac{\alpha_s\left(\mu_R^2\right)}{1 + \alpha_s\left(\mu_R^2\right)\beta_0 \ln\left(Q^2/\mu_R^2\right)}. \tag{2.1}$$

[1] The dependence on $\mu_R$ is still present when truncating the theoretical calculation at a given order: this introduces an uncertainty on the theory predictions.

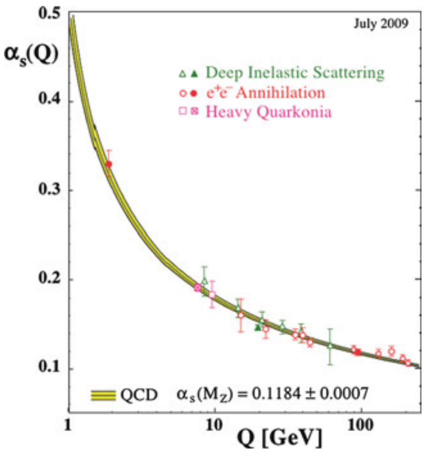


**Fig. 2.2** 2009 world average of running coupling $\alpha_s$ (from [16])

The coupling constant, initially scale-invariant, becomes a function of the scale of the process: the common terminology used is that the coupling constant *runs* with energy. The theoretical and experimental results for the running coupling constant $\alpha_s$ as of 2009 are shown in Fig. 2.2. Contrary to QED, where the coupling constant increases with the scale of the process ($Q^2$ in Fig. 2.2), gluon self interactions lead the $\beta_0$ function to be negative. The coupling constant therefore is sizeable at low $Q^2$ (leading to confined partons) and decreases as a function of $Q^2$ (leading to asymptotic freedom).

Asymptotic freedom and confinement are therefore deeply linked to the gauge structure of QCD that leads to gluon self interactions. This was demonstrated by Gross and Wilczek in 1973 [14, 15], and recognized with a Nobel prize in 2004.

Confinement and asymptotic freedom have relevant experimental consequences: quarks and gluons require interactions with high energy probes to be ejected from the nucleon, and they cannot be observed directly. What one detects instead of quarks and gluons are collimated showers of particles. These particles are the product of a series of steps, summarised as follows in the case of a hadronic collision event following Ref. [17] and pictured in Fig. 2.3:

1. Two hadrons (that can be seen as 'bags of partons' as in the parton model) collide with a large momentum transfer;
2. Two partons (called *incoming* partons) from the hadrons collide and produce the hard process, leaving behind other partons (*outgoing* hadron remnants) and the products of other secondary collisions (multiple interactions).
3. Since electromagnetic and color charges interact, the incoming and outgoing partons can radiate (e.g. a quark can radiate a gluon). These processes can be described using perturbative QCD as outlined in Sect. 2.2.2.
4. When partons are sufficiently 'far' from each other, the coupling becomes strong and confinement plays a part. Being a non-perturbative process, the behaviour of the color force in this situation cannot be described using first principles in

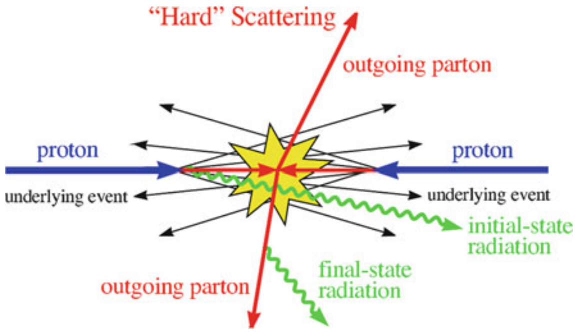


**Fig. 2.3** Schematic representation of a parton–parton collision, leading to a 2→2 scattering event (from [18])

QCD. A simplified picture models the color force as that in a string with a linearly rising potential as charges become separated. The two extremities of the string are the opposite color charges. If the string is extended too much, it will break and create two additional color charges at the endpoints. If two opposite color charges are found close to each other, they will recombine and create a hadron that is observed in the final state. The creation of hadrons as a consequence of confinement is called hadronisation.

The products of the collision that are not directly identified with the hard products of the collision (hadron remnants, products of multiple parton interactions, radiation) are conventionally defined as *underlying event*. Further details on the simulation of these processes are given in Sect. 2.4.2.

### 2.2.2 *Renormalisation, Scale Violations and Parton Distribution Functions*

Asymptotic freedom allows QCD to be described using point-like constituents at sufficiently large energies. The first evidence of this behaviour was given by the SLAC-MIT experiments and interpreted by Feynman and Field using the so-called *parton model* [11]. On the other hand, the momentum scale introduced by renormalisation needed to be accommodated: the *improved parton model* was developed [19, 20]. Starting from these ideas, the perturbative evolution of the quark and gluon behaviour can be predicted separately from the soft, non-perturbative physics, allowing for theoretical calculation of QCD processes.

The differential cross section for lepton–hadron ($lh$) inelastic scattering (as in the SLAC experiments) can be parameterised starting from that of elastic scattering of fundamental particles. Equation 2.2 makes use of *structure functions* $F$ that encapsulate the lack of knowledge on the nucleon behaviour, the kinematics of the scattering (in terms of the momentum transfer $Q^2$ and of the functions $f(y)$ and $g(y)$ that depend on the kinematics of the scattering). It also introduces the variable $x$ that (at leading order) represents the fraction of hadron momentum taken by the struck quark:

$$\frac{d^2\sigma(lh)}{dx dQ^2} = \frac{1}{Q^4}(f(y)xF_1(x, Q^2) + g(y)F_2(x, Q^2)) \tag{2.2}$$

In comparison with the formula of the cross section for incoherent scattering, where each quark composing the hadron can be struck independently from the others, one finds that:

1. the structure function $F_2$ can be identified with the sum of the products of the quark charge squared $e_i^2$ and momentum distribution $xq_i(x)$ for all the quarks in the hadron. The $q_i(x)$ functions can be interpreted (at leading order of perturbation theory) as the probability densities of finding a quark with flavour $i$ carrying a fraction $x$ of the hadron momentum. The momentum distribution for a given quark or gluon is also called parton distribution function, or PDF.

$$F_2^{lh} = \sum_i^{N_q} e_i^2 x q_i(x) \tag{2.3}$$

   The independence of the structure function from momentum transfer $Q^2$ at fixed values of $x$ is known as Bjorken scaling.
2. the two structure functions are not independent if quarks have spin 1/2 (Callan-Gross equation).

The experimental verification of both approximate Bjorken scaling and the Callan-Gross relation in the measurement of the structure functions performed at SLAC shows that quarks in hadrons can be treated as quasi-free spin 1/2 particles. This forms the basis of the quark parton model. Other structure functions, defined as combinations of the quark PDFs, have been derived and measured in data (for a review, see Chap. 5 of Ref. [21]).

When integrating $F_2$ over all possible momentum fractions, only about half of the total hadron momentum is carried by quarks. Probability conservation requires that the area of the total momentum distributions in the proton is equal to unity (this requirement is also called *momentum sum rule*). This calls for the presence of gluons, later observed at the PETRA collider [22]. Gluons are responsible for quark interactions, since they are the carriers of strong force.

Conventionally, partons composing a hadron are divided between gluons, valence quarks and sea quarks. Valence quarks are responsible for the hadron's quantum numbers, while sea quarks are quark/antiquark pairs that can be generated thanks to quantum fluctuations.

Interactions among the partons lead to deviation from the naive parton model in terms of scaling violations, as shown in Fig. 2.4 where experimental points at the same value of $x$ do depend on $Q^2$. Intuitively, an increase in $Q^2$ can be seen as an increase in the resolving power of the probe: if the internal structure of the hadron can be probed at smaller distances, then the number of partons 'seen' increases given that gluons can produce quark/antiquark pairs and quarks or antiquarks can radiate gluons. The DGLAP formalism [24] models these interactions through *splitting functions*

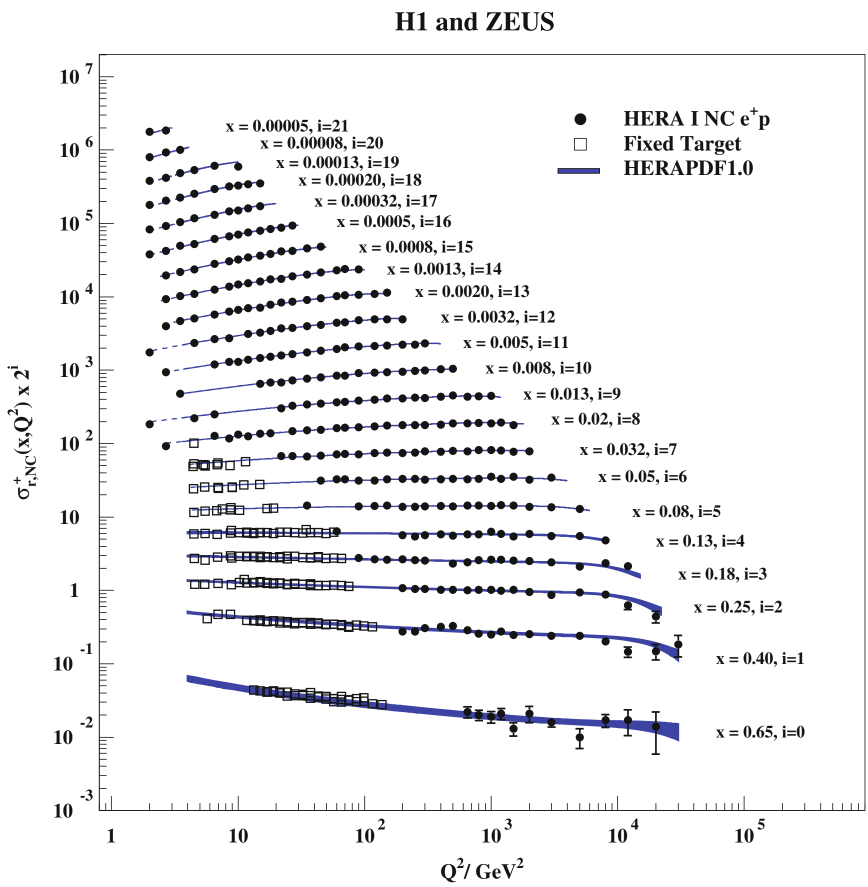


**Fig. 2.4** Measurement of the structure function $F_2$ from the HERA experiments (Figure from [23])

and uses them to evolve perturbatively the renormalised parton densities that contain the $Q^2$ dependence. Given that quarks and gluons interact, the DGLAP equations that describe the change in quark, antiquark and gluon densities with $Q^2$ are coupled. The DGLAP formalism only gives information on the evolution of the PDF, not on their shape, which is derived using a combination of the experimental data on the structure functions and an initial analytical form, as discussed in the next section.

#### 2.2.2.1 PDF Parameterisations

Structure functions such as $F_2$, introduced in the previous section, can be measured experimentally. Parton distribution functions are not observable, but instead they are extracted using combinations of measurements for independent structure functions. *Sum rules* that constrain groups of PDF (e.g. on the consistency of the quantum numbers of the hadron) can also be used to infer information on parton distribution functions. Details on the extraction of PDF parameters are given in Chap. 8.

One essential ingredient for the extraction of parton distribution functions is the parameterisation of the PDFs at a starting scale. Since such a parameterisation is not predictable from first principles in QCD, simple considerations on the behaviour of the functions and assumptions on their shapes need to be introduced. For nucleons, the valence quark PDFs should be allowed to peak around 1/3 (in the assumption that the three valence quarks will share equal fractions of the hadron momentum), with an additional smearing due to the intrinsic parton momentum and the presence of sea quarks. One also expects that sea quarks will grow for lower values of $x$ because of the divergent nature of QCD radiation and because gluons branch into $q\bar{q}$ pairs. Valence quarks will not have this behaviour because gluon interactions will not change the quark flavour. Furthermore, the parameterisations must respect the kinematic of the $x$ variable: $0 < x < 1$. This leads to the following basic parameterisations for the PDFs:

$$xV(x) = Ax^B(1-x)^C \tag{2.4}$$

The behaviour at high $x$ can also be predicted using what is called the *spectator model* [25], while the power-law behaviour for $x \to 0$ can be predicted using Regge trajectories [26].

The exact starting scale parameterisations used by the different groups that extract parton distribution functions vary, and those used for this thesis are detailed in Chap. 8.

### *2.2.3 QCD Factorisation*

One of the reasons of the success of QCD as a predictive theory is that the short-distance component of the scattering process described by perturbative QCD can be separated from the non-perturbative long-distance component: this result is known as the factorisation theorem [27]. Factorisation implies that perturbation theory can be used to calculate the hard scattering cross section, while universal functions such as the PDFs can be included a posteriori to obtain the full theoretical prediction. This is shown in Eq. 2.5 using the quantities in Fig. 2.5 for a hard hadronic process:

$$\begin{aligned} d\sigma_{hard}(p_A, p_B, Q^2) = \sum_{ab} \int dx_a dx_b f_{a/A}\left(x_a, \mu_F^2\right) f_{b/B}\left(x_b, \mu_F^2\right) \\ \times d\hat{\sigma}_{ab\to cd}\left(\alpha_s\left(\mu_R^2\right), Q^2/\mu_R^2\right). \end{aligned} \tag{2.5}$$

$f_{a/A}$ and $f_{b/B}$ are the parton momentum densities for the two interacting partons $a, b$ with respect to hadrons $A, B$. Since factorisation is a byproduct of a procedure that absorbs singularities into physical quantities in the same fashion as renormalisation,

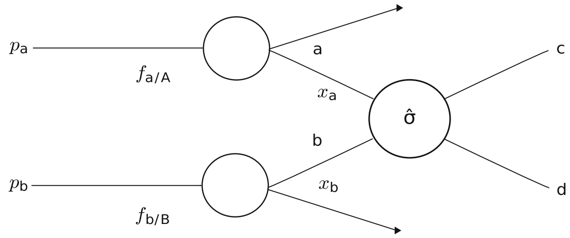


**Fig. 2.5** Schematic illustration of hard hadronic process (Figure from [21])

a new scale $\mu_F^2$ is introduced. When truncating calculations at a given order, the uncertainties due to the choice of scale need to be calculated in order to account for higher order terms.

Factorisation is related to the connection of inclusive hadronic observables to the underlying kinematics of the hard scattering of quarks and gluons, even when the final signature is influenced by parton distribution functions, fragmentation and hadronisation.

Factorisation and the comparison of experimental data from different processes indicate that the parton distribution functions are universal (i.e. they do not depend on the physics process). They can be derived from different physics processes and then used to derive full theoretical predictions independently from the calculation of the hard scattering cross section. The universality of parton distribution functions is confirmed by the comparison of the extraction of the structure functions from different processes as mentioned in Sect. 2.2.2.

## 2.3 Infrared Safety in Inclusive Processes: Jets

QCD cross sections diverge when calculating processes that involve the radiation of infinitely soft particles (infrared divergencies) and when radiation happens at small angle (collinear divergences). However, infrared divergences cancel by virtue of the Kinoshita–Lee–Nauenberg theorem [28, 29]. The practical consequence of this theorem is that observables that are inclusive enough to be insensitive to processes that distinguish between different numbers of partons are *infrared safe* and are not affected by infrared divergences. This is mirrored by the behaviour of experimental measurements: detectors have a finite spatial resolution and will not be able to resolve the products of separate partons.

If the objects that represent partons in the final state have a well defined behaviour both in theory and experiments, then the parton kinematics will be reflected in the kinematic of the final state object. This is where the definition of *jets* becomes indispensable for QCD measurements. A jet can be naïvely seen as a group of collimated particles generated by the hadronisation of a parton in the scattering process, as shown schematically in Fig. 2.6.

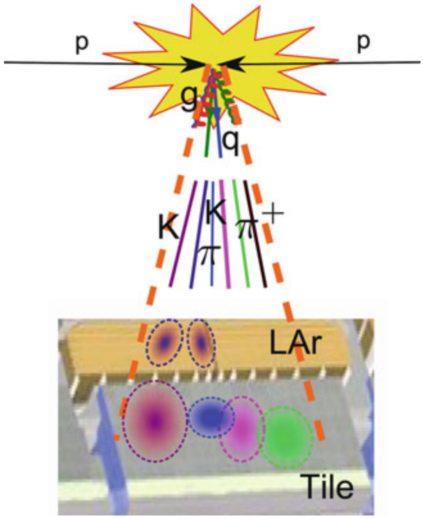


**Fig. 2.6** Development of a jet: collimated particles from the hadronisation of quarks and gluons deposit energy in the ATLAS calorimeters, as described in Chap. 3

The concept of jets was introduced even before QCD was formalised (see for example Ref. [30]). A rigorous definition of jets for use as a connection between perturbative QCD and observable hadronic final state was introduced by Sternman and Weinberg [31]. Given that thanks to momentum conservation two partons with sufficiently high transverse momenta will be produced back to back, one can define a jet cross section by including all partons and their radiation if they are found in two cones of opening angle $\delta$. These cones will only leave out a finite amount of energy $\epsilon$. The definition of boundaries for the integration in terms of $\delta$ and $\epsilon$ allows for a finite cross section. A similar algorithm can also be used when dealing with the two collimated sprays of particles produced by the hadronisation of the partons. Different infrared and collinear safe algorithms have since been introduced, but what remains of this interpretation is the requirement of using the same jet finding algorithm in theory and experiment to be able to compare theoretical prediction to data. More details on the definition of jets and the algorithms used for jet finding are given in Chap. 4.

### *2.3.1 Inclusive Jet Production*

The inclusive jet cross section is a standard tool to test perturbative QCD at hadron colliders, spanning over numerous orders of magnitude in terms of the jet transverse momentum. The experimental measurement does not present particular difficulties in terms of background subtraction given that jets are the predominant hard process produced in the hadron–hadron collisions.

Jets are dominantly produced through scattering of two partons (gluon–gluon, quark–gluon or quark–antiquark) leading to two partons in the final state.

As mentioned in Sect. 2.2, asymptotic freedom and factorisation allow the calculation of theoretical predictions for QCD processes using perturbation theory. The difficulty of theoretical calculations increases with the order of perturbation, corresponding to the number of partons involved. At leading order only two initial and final state partons are involved. For each increasing order of perturbation theory, one parton needs to be added to the $2 \rightarrow 2$ process, either as a 'leg' or as a 'loop', and the diagrams will interfere in the calculation. The theoretical prediction for the inclusive jet cross section is known at next to leading order (NLO) in perturbation theory.

### *2.3.2 Motivations to Measure the Inclusive Jet Cross Section*

Jets are a necessary ingredient for many analyses at a hadron collider. Measuring the inclusive cross section requires a detailed understanding of jets and the related systematic uncertainties. Since the theory/data comparison for the inclusive jet cross section in measurements prior to the one detailed in this thesis showed excellent agreement, as in Refs. [32] and [33], an early data/theory comparison can be performed in a kinematic region where agreement has been previously found to ensure that jets in ATLAS are well understood.

Furthermore, a measurement of the jet cross section with the data collected by the ATLAS detector in the first year of operation of the Large Hadron Collider spans kinematic regions that were previously unexplored, and it can be used as a more stringent test of perturbative QCD over phase space. If the experimental and theoretical uncertainties are small enough and well understood, the measurement can also be used to constrain the parton distribution functions exploiting the extended kinematic range, especially the gluon distribution at values of $x$ up to 0.2.

This topic will be developed further in Chap. 8.

## 2.4 Theoretical Tools

A theoretical prediction is fully comparable to data when corrections are applied to the calculation to simulate additional orders in perturbation theory and non perturbative effects, and after all detector-specific effects have been removed from the experimental measurement. The tools used to calculate the NLO theoretical prediction, for the extraction of jet calibration parameters and for the theory/data comparison of the measurement of the inclusive jet cross section detailed in this thesis are listed in the following paragraphs.

### 2.4.1 NLO Calculation Software and Convolution with PDFs

The next to leading order calculation for the hard process is performed using the NLOJET++ 4.1.2 [34] software. This result needs to be convoluted with the parton distribution functions at given renormalisation and factorisation scales: this is achieved with the APPLGrid software [35]. APPLGrid allows for a posteriori inclusion of PDF and process scales, so that the time-consuming calculation of the next to leading order coefficients only need to be evaluated once. This is particularly useful when systematic uncertainties derived from variations of the PDFs, scales and strong coupling constant need to be estimated.

### 2.4.2 Parton Shower Monte Carlo Generators

Monte Carlo event generators such as PYTHIA [36] and ALPGEN [37] are employed to simulate inclusive QCD jet events from proton–proton collisions when the information on the particles entering the detector after hadronisation is needed.

These generators simulate the entire QCD event, using various models to simulate the non-perturbative steps mentioned in Sect. 2.2.1. No full calculation beyond leading order is employed in the generators that are normally used, although the ALPGEN generator is able to provide matrix elements for up to 6 additional partons as 'legs' of the diagram. After the hard scattering ($2 \rightarrow 2$, or $2 \rightarrow n$) is simulated starting from the matrix element calculation that includes the convolution with a PDF of choice, subsequent radiation is simulated using a series of probabilities for partons to split. This approach is called *parton shower*, and it needs to be matched to the matrix element calculation to avoid double counting of radiation generated by both the hard scattering and by the parton shower. The splittings are iterated until a cut-off scale is reached (usually 1 GeV), and at that point hadronisation will start. These generators will have specific models (or employ external plug-ins) for hadronisation and multiple parton interactions, whose parameters can be tuned using specific data.

The Monte Carlo generators used in the inclusive jet analysis are listed below, together with their main characteristics and choices of PDF and tunes.

PYTHIA simulates non-diffractive proton-proton collisions using a $2 \rightarrow 2$ matrix element at leading-order of the strong coupling to model the hard subprocess, and use parton showers to model additional radiation in the leading-logarithmic approximation using $p_T$-ordering [38]. The hadronisation model used is an evolution of the string model described in Sect. 2.2.1 (Lund string model [39]). Multiple parton interactions are also simulated within PYTHIA [38]. The PDF used for the PYTHIA samples is the modified leading order set MRST LO* [40]. Modified leading order PDFs can be used in combination with a leading order generator to obtain a result qualitatively similar to what one would obtain with a next to leading order calculation.[2]

ALPGEN is a leading order matrix-element generator for hard multi-parton processes in hadronic collisions [37]. It is interfaced to the HERWIG generator to produce angular-ordered parton showers in leading-logarithmic approximation [41]. Parton showers are matched to the matrix element with the MLM matching scheme [42]. The hadronization is simulated in HERWIG [41] using the cluster model [43] where gluons split in $q\bar{q}$ pairs that are subsequently regrouped into colorless clusters to produce hadrons. Multiple parton interactions are modelled using JIMMY [44]. The PDF used for the ALPGEN samples is CTEQ6L1 [45].

HERWIG++ [46] is a multipurpose event generator built on the experience of HERWIG. It simulates the full hadronic interaction in a similar fashion as PYTHIA, but using angular ordering in the generation of the parton shower and specific hadronisation and multiparton interactions models [47]. The MRST LO* PDF set is used in combination with the HERWIG++ generator.

The parameters used for tuning the underlying event models in the PYTHIA and HERWIG event generators have been derived from minimum bias measurement in ATLAS data [48, 49] and are denoted as ATLAS MC10 tune.

#### 2.4.2.1 Nominal Monte Carlo Sample

The baseline Monte Carlo sample used in this analysis for the calibration and derivation of the jet energy scale and its uncertainty is generated with PYTHIA and will be referred to as *nominal sample* in the following. The full sample[3] is composed of 12.6 million simulated PYTHIA QCD jet events. Due to the steeply falling jet cross section, the samples have been generated in 9 bins of transverse momentum of the outgoing partons in the $2 \rightarrow 2$ hard scattering process ($\hat{p}_T$), covering the range 8 GeV–3.5 TeV. Each sub-sample is weighted according to its cross section to form the final event sample. The sample used for the theory/data comparisons and for the derivation of the non perturbative corrections that need to be applied to the NLO calculation includes the nominal PYTHIA sample, complemented by a minimum bias sample of approximately 20 million events for jets with $\hat{p}_T$ below 8 GeV. Events with $\hat{p}_T$ below 17 GeV are taken from the minimum bias sample, while events above this threshold are taken from the nominal sample mentioned above.

The PYTHIA QCD jet sample has been validated with data collected by the ATLAS detector at $\sqrt{s} = 900$ GeV and $\sqrt{s} = 7$ TeV [50–57]. Jets measured in ATLAS are reasonably well described by the Monte Carlo simulation, before and after their calibration, as shown in Fig. 2.7.

[2] This statement is currently being tested in a number of measurements at LHC energies.

[3] The calibration has been derived on a smaller sample of 3.6 million events.

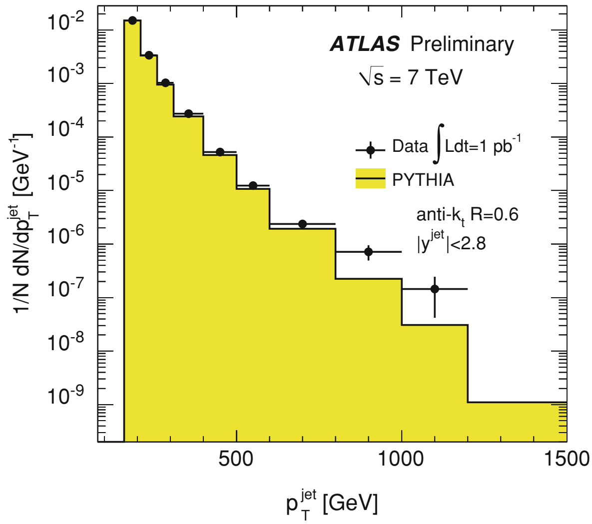


**Fig. 2.7** Observed inclusive jet $p_T$ distribution (*black dots*) for anti-$k_t$ $R = 0.6$ jets (as defined in Chap. 4) with $p_T > 160\,\text{GeV}$ and pseudorapidity $|y| < 2.8$ compared to the Monte Carlo prediction from the nominal sample (*yellow* histogram). The distribution is normalized to unity and only statistical uncertainties are included

## References

1. G. Altarelli, The standard model of particle physics, arXiv:0510281 [hep-ph] (To appear in the ‘Encyclopedia of Mathematical, Physics, Elsevier’).
2. C. Quigg, Unanswered questions in the electroweak theory. arXiv:0905.3187 [hep-ph]. arXiv:0905.3187v1 [hep-ph]. <!– Missing/Wrong Year –>
3. W. Burcham, M. Jobes, *Nuclear and Particle Physics* (Longman, Singapore, 1995)
4. R.K. Ellis, W.J. Stirling, B.R. Webber, *QCD and Collider Physics (Cambridge Monographs on Particle Physics, Nuclear Physics, and Cosmology)* (Cambridge University Press, Cambridge, 2003)
5. P. Higgs, Broken symmetries, massless particles and gauge fields. Phys. Lett. **12**(2), 132–133 (1964)
6. F. Englert, R. Brout, Broken symmetry and the mass of Gauge vector mesons. Phys. Rev. Lett. 13 (1964) 321–323. http://link.aps.org/doi/10.1103/PhysRevLett.13.321
7. Wikipedia (adapted by C. Fitzpatrick) (2009) Standard model–wikipedia, the free encyclopedia, online. http://en.wikipedia.org/w/index.php?title=Standard_Model. Accessed 6 June 2009
8. H. Yukawa, On the interaction of elementary particles. I*, Progr. Theor. Phys. Suppl. 1, 1–10 (1955).http://ptp.ipap.jp/link?PTPS/1/1/
9. C.N. Yang, R.L. Mills, Conservation of isotopic spin and isotopic Gauge invariance. Phys. Rev. **96**(1), 191–195 (1954)
10. M. Gell-Mann, Y. Ne’eman, *The Eightfold Way: With New Contributions from the Authors* (Advanced Book Classics (Perseus Publishing, Cambridge, 2000)
11. R. Feynman, *Photon-Hadron Interactions* (Reading, Advanced Book Classics (Addison-Wesley, 1998)
12. R. Cahn, G. Goldhaber, *The Experimental Foundations of Particle Physics* (Cambridge University Press, Cambridge, 2009)

13. D.J. Gross, The discovery of asymptotic freedom and the emergence of QCD. Proc. Natl. Acad. Sci. U S A 102(26), 9099–9108, (2005). http://www.pnas.org/content/102/26/9099.full.pdf+html
14. D.J. Gross, F. Wilczek, Asymptotically free Gauge theories. I, Phys. Rev. D 8(10), 3633–3652 (1973).
15. D.J. Gross, F. Wilczek, Asymptotically free gauge theories. II, Phys. Rev. D 9(4), 980–993 (1974).
16. S. Bethke, The 2009 world average of $\alpha_s(M_Z)$, Eur. Phys. J. C 64, 689–703 (2009). arXiv:0908.1135 [hep-ph].
17. T. Sjostrand, Monte Carlo generators. arXiv:0611247 [hep-ph]. <!– Missing/Wrong Year –>
18. J.M. Campbell, J.W. Huston, W.J. Stirling, Hard interactions of quarks and gluons: a primer for LHC physics. Rept. Prog. Phys. 70 89 (2007). arXiv:0611148 [hep-ph].
19. J.C. Collins, D.E. Soper, G.F. Sterman, Factorization of hard processes in QCD. Adv. Ser. Direct. High Energy Phys. 5, 1–91 (1988). arXiv:0409313 [hep-ph].
20. R.K. Ellis, H. Georgi, M. Machacek, H.D. Politzer, G.G. Ross, Perturbation theory and the parton model in QCD. Nucl. Phys. B **152**(2), 285–329 (1979)
21. R. Devenish, A. Cooper-Sarkar, Deep Inelastic Scattering (Oxford University Press, Oxford, 2004). http://books.google.com/books?id=L68zn24GgkcC
22. P. Söding, On the discovery of the gluon. Eur. Phys. J. H. **35**(1), 3–28 (2010). doi:10.1140/epjh/e2010-00002-5
23. H1 and ZEUS Collaboration, F.D. Aaron et al., Combined measurement and QCD analysis of the inclusive ep scattering cross sections at HERA. JHEP 01, 109 (2010). arXiv:0911.0884 [hep-ex].
24. G. Altarelli, G. Parisi, Asymptotic freedom in parton language. Nucl. Phys. B **126**(2), 298–318 (1977)
25. S.J. Brodsky, G.R. Farrar, Scaling laws for large-momentum-transfer processes. Phys. Rev. D **11**(5), 1309–1330 (1975)
26. F.J. Gilman, Photoproduction and electroproduction. Phys. Rep. C **4**, 96–151 (1972)
27. J.C. Collins, D.E. Soper, The theorems of perturbative QCD. Annu. Rev. Nucl. Part. Sci. **37**(1), 383–409 (1987)
28. T.D. Lee, M. Nauenberg, Degenerate systems and mass singularities. Phys. Rev. **133**, B1549–B1562 (1964)
29. T. Kinoshita, Mass singularities of Feynman amplitudes. J. Math. Phys. **3**, 650–677 (1962)
30. S.D. Drell, D.J. Levy, T.-M. Yan, Theory of deep-inelastic lepton-nucleon scattering and lepton-pair annihilation processes. III. Deep-inelastic electron-positron annihilation, Phys. Rev. D 1(6), 1617–1639 (1970).
31. G. Sterman, S. Weinberg, Jets from quantum chromodynamics. Phys. Rev. Lett. **39**(23), 1436–1439 (1977)
32. CDF Collaboration, T. Aaltonen et al., Measurement of the inclusive jet cross section at the fermilab tevatron p-pbar collider using a cone-based jet algorithm, Phys. Rev. D 78 052006, (2008). arXiv:0807.2204 [hep-ex].
33. D0 Collaboration, V. Abazov et al., Measurement of the inclusive jet cross-section in $p\bar{p}$ collisions at $s^{1/2}$ =1.96-TeV. Phys. Rev. Lett. 101 062001 (2008). arXiv:0802.2400 [hep-ex].
34. Z. Nagy, Next-to-leading order calculation of three jet observables in hadron hadron collision. Phys. Rev. D 68 094002 (2003). arXiv:0307268 [hep-ph].
35. T. Carli et al., A posteriori inclusion of parton density functions in NLO QCD final-state calculations at hadron colliders: the APPLGRID project. Eur. Phys. J. C 66, 503–524 (2010). arXiv:0911.2985 [hep-ph].
36. T. Sjostrand, S. Mrenna, P.Z. Skands, PYTHIA 6.4 physics and manual. JHEP 05, 026 (2006). arXiv:0603175 [hep-ph].
37. M.L. Mangano, M. Moretti, F. Piccinini, R. Pittau, A.D. Polosa, ALPGEN, a generator for hard multiparton processes in hadronic collisions. JHEP 07, 001 (2003). arXiv:0206293 [hep-ph].
38. T. Sjostrand, P.Z. Skands, Transverse-momentum-ordered showers and interleaved multiple interactions. Eur. Phys. J. C 39, 129–154 (2005). arXiv:0408302 [hep-ph].

39. B. Andersson, G. Gustafson, G. Ingelman, T. Sjöstrand, Parton fragmentation and string dynamics. Phys. Rep. **97**, 31–145 (1983)
40. A. Sherstnev, R.S. Thorne, Parton distributions for LOgenerators. Eur. Phys. J. C 55, 553–575 (2008). arXiv:0711.2473 [hep-ph].
41. G. Corcella et al., HERWIG 6.5 release note, arXiv:0210213 [hep-ph].
42. M.L. Mangano, M. Moretti, R. Pittau, Multijet matrix elements and shower evolution in hadronic collisions: $Wb\bar{b} + n$ jets as a case study. Nucl. Phys. B 632, 343–362 (2002). arXiv:0108069 [hep-ph].
43. B.R. Webber, A QCD model for jet fragmentation including soft gluon interference. Nucl. Phys. B **238**(3), 492–528 (1984)
44. J.M. Butterworth, J.R. Forshaw, M.H. Seymour, Multiparton interactions in photoproduction at HERA. Z. Phys. C 72, 637–646 (1996). arXiv:9601371 [hep-ph].
45. J. Pumplin et al., New generation of parton distributions with uncertainties from global QCD analysis. JHEP 07, 012 (2002). arXiv:0201195 [hep-ph].
46. M. Bahr, S. Gieseke, M. Gigg, D. Grellscheid, K. Hamilton, et al., Herwig++ physics and manual. Eur. Phys. J. C 58, 639–707 (2008). arXiv:0803.0883 [hep-ph].
47. M. Bahr, S. Gieseke, M.H. Seymour, Simulation of multiple partonic interactions in Herwig++, JHEP 0807, 076 (2008). arXiv:0803.3633 [hep-ph].
48. ATLAS Collaboration, Charged particle multiplicities in pp interactions at $\sqrt{s}$ = 0.9 and 7 TeV in a diffractive limited phase-space measured with the ATLAS detector at the LHC and new PYTHIA6 tune, ATLAS-CONF-2010-031, CERN, Geneva, May 2010.
49. ATLAS Collaboration, First tuning of HERWIG/JIMMY to ATLAS data, ATL-PHYS-PUB-2010-014, CERN, Geneva, October 2010.
50. ATLAS Collaboration, Response of the ATLAS calorimeter to single isolated hadrons produced in proton proton collisions a centre-of-mass energy of $\sqrt{s} = 900$ GeV, ATLAS-CONF-2010-017, CERN, Geneva, March 2010.
51. ATLAS Collaboration, ATLAS calorimeter response to single isolated hadrons and estimation of the calorimeter jet scale uncertainty, ATLAS-CONF-2010-052, CERN, Geneva, June 2010.
52. ATLAS Collaboration, Inputs to jet reconstruction and calibration with the ATLAS detector using proton-proton collisions at $\sqrt{s} = 900$ GeV, ATLAS-CONF-2010-016, CERN, Geneva, April 2010.
53. ATLAS Collaboration, Properties and internal structure of jets produced in proton-proton collisions at $\sqrt{s} = 900$GeV, ATLAS-CONF-2010-018, CERN, Geneva, April 2010.
54. ATLAS Collaboration, Observation of energetic jets in pp collisions at $\sqrt{s} = 7$TeV using the ATLAS experiment at the LHC, ATLAS-CONF-2010-043, CERN, Geneva, April 2010.
55. ATLAS Collaboration, Measurement of inclusive jet and dijet cross sections in proton-proton collisions at 7 TeV centre-of-mass energy with the ATLAS detector. Eur. Phys. J. C 71, 1512 (2011). arXiv:1009.5908 [hep-ex].
56. ATLAS Collaboration, Properties of jets and inputs to jet reconstruction and calibration with the ATLAS detector using proton-proton collisions at $\sqrt{s} = 7$ TeV, ATLAS-CONF-2010-053, CERN, Geneva, June 2010.
57. ATLAS Collaboration, In-situ pseudo-rapidity inter-calibration to evaluate jet energy scale uncertainty and calorimeter performance in the forward region, ATLAS-CONF-2010-055, CERN, Geneva, June 2010.

http://www.springer.com/978-3-642-30537-5

Measurement of the Inclusive Jet Cross Section with the
ATLAS Detector at the Large Hadron Collider
Doglioni, C.
2012, XII, 160 p., Hardcover
ISBN: 978-3-642-30537-5